

## Investigation of the Mobilization of Residual Oil Using Micromodels

A. S. Ibrahim, N. S. Abdelfattah, and I. Chatzis

The Petroleum Institute, Petroleum Engineering Program, Abu Dhabi, U.A.E.  
*ahsibrahim@pi.ac.ae, nashabib@pi.ac.ae, ichatzis@pi.ac.ae*

### Abstract

The mobilization of residual oil was investigated in glass micromodels consisting of capillary networks with water-wet wettability as a function of capillary number (ratio of viscous to capillary forces). The micromodels used in this work had variable pore throat and pore body size distribution. Experimental results demonstrated that the entrapped residual oil blobs have a preferable orientation along the macroscopic flow direction of waterflooding. For substantial mobilization of the waterflood residual oil, the corresponding capillary number needs to be 100 times larger than that for the onset of mobilization of the largest blobs in place at the end of waterflooding. The reduced residual oil saturation with increasing capillary number obtained in this study is in qualitative and quantitative agreement with published capillary number curves for water-wet sandstones. A key feature of oil blob mobilization at high capillary number is the break-up of mobilized blobs to sub-pore size droplets as they flow through the pore network, some of which attach to the pore walls and thus making complete mobilization very difficult. It was concluded that glass micromodels offer the potential to screen the best surfactant formulations for EOR application using residual oil mobilization experiments and for displacements of continuous oil in place.

### 1. Introduction

A very significant fraction of the oil initially in place in an oil field is permanently trapped at the end of waterflooding operations. This trapped oil is referred to as waterflood residual oil, which is a strong function of the pore structure heterogeneities, flooding rate and wettability conditions. The residual oil saturation can be 15% of pore volume in homogeneous unconsolidated sands, and as high as 50% of the pore volume in pore systems with vugs and high aspect ratio of pore body size to pore throat size [1-2]. Because of oil shortages globally, abandoned oil fields are revisited by the oil companies to recover this residual oil by applying enhanced oil recovery (EOR) techniques. The waterflood residual oil is recoverable by chemical flooding at high capillary number. The capillary number is defined as the ratio of viscous to capillary forces. A key objective of this work was to develop a better understanding of the residual oil mobilization process and thus improve the design of chemical flooding projects in water-wet and oil-wet reservoirs. Improved oil recovery technologies in the U.A.E. and elsewhere will become a reality very soon, as the producing oil fields will run out of the primary oil recovery phase.

The advancement of knowledge for the pore scale phenomena of oil trapping and oil mobilization mechanisms was made possible based on studies that used micromodels of capillary networks etched on glass. The glass micromodels are made using a microlithography-based technique similar to the making of printed circuits boards and microchip manufacturing. The desired pattern of pore channels is etched on a glass plate using hydrofluoric acid. After inlet and outlet ports are drilled in the etched glass plate, it is fused on to another flat glass plate at 725°C, thus creating a sintered two-dimensional glass micromodel with a capillary network in place between the sintered glass plates. This porous medium can be used for studying immiscible displacements of oil with water injection [1]. An example of a square capillary network and photograph of the selected pores in the micromodel seen under a microscope is shown in Figure 1. As indicated in this figure, the residual oil blobs are found to occupy one to several pores. The pores with residual oil in water-wet media are of generally consisting of predominantly large pore size. The water phase occupies the predominantly smaller pores and the pore corners of space that has residual oil occupancy.

In this study, attention is focused on the mechanisms of oil recovery by waterflooding, and the mobilization of residual oil as a function of flow rate (capillary number). The model was saturated by water first, and the water was then displaced with oil to establish initial oil and connate water conditions. Subsequently, the water was injected at a constant injection rate to waterflood the system and establish the residual oil condition. The magnitude of residual oil was monitored as a function of the water injection rate by video-recording and image analysis of the microscopic state of residual oil blobs. After a displacement condition, a photograph was taken and the amount of residual oil was determined by image analysis. A commercially available image analysis software, Image Tool, was used for quantitative measurements.

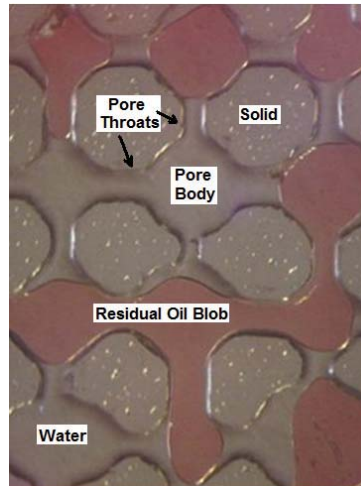


Figure 1. Portion of the micromodel SRC-1 and residual oil blobs seen after waterflooding.

## 2. Theory

The mobilization of trapped residual oil requires the viscous forces across the length of a blob to exceed the capillary forces. Consider the oil blob in a simplified pore network illustrated in Figure 2 with water-wet characteristics. The pressure difference in the water phase from point A to point B must become greater than the difference between the drainage capillary pressure at position 1 and the imbibitions capillary pressure at position 2, for the oil blob to mobilize in the downstream pore at position B. Expressing the capillary pressure using the pore constriction size at location 1 and the pore body size at location 2, we can write [1]:

$$(P_{w,A} - P_{w,B}) = \Delta P_m; \text{ and } \Delta P_m \geq \left( \frac{4\sigma_{ow} \cos \theta_R}{D_1} - \frac{4\sigma \cos \theta_A}{D_2} \right) \quad (1)$$

where  $\Delta P_m$  is the required mobilization pressure difference,  $\sigma_{ow}$  is the oil-water interfacial tension,  $D_1$  and  $D_2$  are the pore throat and pore body diameter respectively,  $\theta_R$  is the receding contact angle, and  $\theta_A$  is the advancing contact angle.

The Darcy velocity of the water phase with the residual oil present is governed by Darcy's law:

$$v_w = \frac{Kk_{rw}}{\mu_w} \frac{\Delta P_w}{L} \quad (2)$$

where  $v_w$  is the Darcy velocity of water,  $\mu_w$  is the viscosity of water,  $\Delta P_w/L$  is the macroscopic pressure gradient,  $K$  is the absolute permeability and  $k_{rw}$  is the relative permeability to water. By equating the macroscopic pressure gradient with the capillary pressure difference across the blob divided by the blob length  $l_{blob}$ , then we have:

$$\frac{\Delta P_w}{L} = \frac{1}{l_{blob}} \left( \frac{4\sigma_{ow} \cos \theta_R}{D_1} - \frac{4\sigma_{ow} \cos \theta_A}{D_2} \right) \quad (3)$$

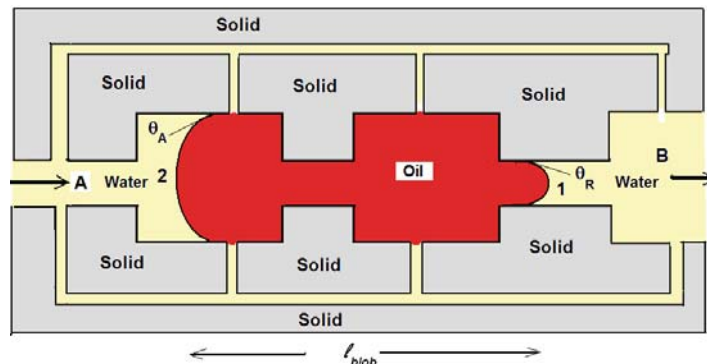


Figure 2. A schematic of an oil blob trapped in a water-wet capillary network.

Let

$$\lambda = \frac{\ell_{blob}}{D_1} \text{ and } \beta = \frac{D_2}{D_1} \quad (4)$$

Using the above definitions, Equation (3) can be re-arranged as:

$$\frac{\Delta P_w}{L} = \frac{4\sigma_{ow}}{\lambda D_1^2} \left( \cos\theta_R - \frac{\cos\theta_A}{\beta} \right) \quad (5)$$

From the above equation, we see that the macroscopic pressure gradient required for mobilization is proportional to the interfacial tension and is inversely proportional to the product of blob length times the pore throat diameter. The larger the interfacial tension, the larger the required pressure gradient for mobilization. On the other hand, the longer the blob length, the smaller the required pressure gradient for mobilization. The pore body to pore throat size ratio is referred to as the aspect ratio,  $\beta$ . This aspect ratio is also an important pore structure parameter. All other parameters being the same, the larger the aspect ratio, the larger the pressure gradient required for oil blob mobilization. If one combines Equation (5) with Equation (2), the following dimensionless expression, known as capillary number, can be obtained [2]:

$$\frac{v_w \mu_w}{\sigma_{ow}} = \frac{Kk_{rw}}{\sigma_{ow}} \frac{\Delta P_w}{L} = 4 \left( \frac{Kk_{rw}}{\lambda D_1^2} \right) \left( \cos\theta_R - \frac{\cos\theta_A}{\beta} \right) \quad (6)$$

The capillary number is a ratio of viscous forces to capillary forces. The relative permeability function for the relative permeability to water,  $k_{rw}$ , can be expected to be constant at a given saturation condition for systems having similar pore geometry [3]. Therefore, the macroscopic pressure gradient for the flow of water in systems having the same residual oil saturation is proportional to  $(1/K)$ ,  $K$  being the absolute permeability. For geometrically similar systems such as cubic networks consisting of pore bodies interconnected with pore throats of size  $D_1$ , the absolute permeability is approximated by [2,3]:

$$K = \frac{\phi D_1^2}{96} \quad (7)$$

where  $\phi$  is the porosity. By substituting the  $D_1^2$  by  $(96K/\phi)$ , and the macroscopic pressure gradient by  $\Delta P_w / L = \Delta P_m / l_{blob}$ , it can be found by algebraic manipulations using Equation (6) that:

$$\frac{K \Delta P}{L \sigma_{ow}} = \frac{4\phi}{96\lambda} \left( \cos\theta_R - \frac{\cos\theta_A}{\beta} \right) \quad (8)$$

where  $\Delta P$  is the pressure difference between the inlet pressure and exit pressure of a porous medium of length  $L$  in residual oil mobilization tests. The relation of residual oil saturation (ROS) in a porous medium as a function of capillary number is known as the capillary number curve. Based on Equation (8), systems that have the same wettability characteristics and microstructure of residual oil will be described by the same capillary number curve. However, variation in the shape of the capillary number curve will reflect variation in pore geometry indicated by the values of  $\phi$  and  $\beta$  from a sample to sample, and likely associated differences due to blob size distribution, which is captured by parameter  $\lambda$ .

### 3. Experimental details

Capillary number correlations for the mobilization of residual oil from water media are already available in the published literature for core samples of sandstone reservoir rocks. In the present study however, it was desirable to determine how representative are the pore network micromodels etched on glass as porous media models to describe the capillary number curves for the following two cases: a) the mobilization of waterflood residual oil, and b) the displacement of initially continuous oil phase as a function of capillary number. Furthermore, the visualization of the residual oil microstructure with capillary number in micromodels was another objective to provide experimental evidence of the break-up of the oil blobs during the residual oil mobilization process.

#### 3.1 Porous media and fluids used

Two glass micromodels of pore networks with a square lattice topology having different pore structure at the pore scale were utilized as test porous media. Details of the fabrication technique of two-dimensional network micromodels etched on glass are given elsewhere [1]. Pictures of sections of them appear in photographs of waterflooding tests performed as indicated in the various figures that appear in

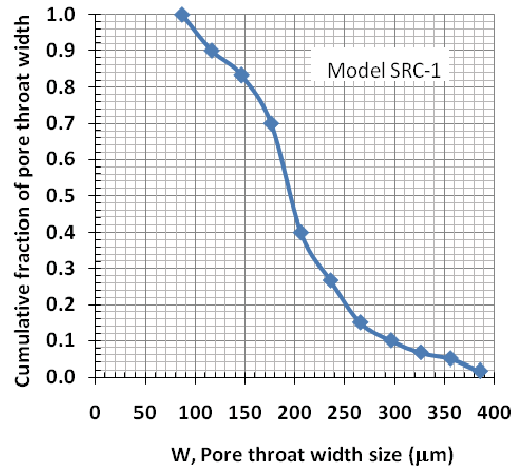


Figure 3. Cumulative fraction of Pore throats with width greater than specified with size in micromodel SRC-1.

this paper. The glass micromodels are known to have water-wet characteristics in waterflooding tests. The fluids used in this study were kerosene with a red dye added to it to simulate the “crude oil” for visualization and de-ionized water that was used for the displacement of oil. The interfacial tension  $\sigma_{ow}$  is about 26mN/m for the dyed oil-water system and about 3mN/m when using water with soap.

The pore bodies in the pore network serve as the pore junctions that are interconnected with pore throats. The pore bodies were made to have different sizes, thus having a distribution of aspect ratio values. Using high resolution images, the width of a pore throat seen on a picture of the micromodel were determined by image analysis for their width size and size distribution. The cumulative pore throat width distribution is shown in Figure 3 for micromodel SRC-1. This micromodel (SRC-1) had a length of 102 mm and width of 44mm (87 pores long by 41pores wide) and a pore volume of 350 $\mu$ L. The second micromodel (SX-4) had a width of 46 mm, length of 80 mm and pore volume of 250  $\mu$ L. The pore volume was determined gravimetrically by measuring the weight of saturated micromodel with water minus the dry weight of micromodel. The absolute permeability to water was measured by the falling head permeameter method [3] and the two models had similar permeability values (20-23 $\mu$ m<sup>2</sup>).

### 3.2 Immiscible Displacements

Two types of oil displacement experiments were performed: a) the mobilization of residual oil experiment, and b) the displacement of initially oil continuous phase as a function of capillary number. The experimental procedure for the mobilization experiments was as follows:

- **Step 1:** The micromodel was first saturated with water and the micromodel was then oil-flooded to establish high initial oil saturation by flowing 10cm<sup>3</sup> of oil at 20cm<sup>3</sup>/min.
- **Step 2:** Normal waterflood residual oil saturation was established by water injection at low flow rate (0.01cm<sup>3</sup>/min) using a constant rate syringe metering pump (After water-breakthrough, the residual oil remained in place without any sign of mobility and a picture was taken. The picture was analyzed to determine the area occupied by the residual oil in the pore network. This area was used as the reference area to denote the normal waterflood residual oil saturation ( $S_{or}^*$ ) in the micromodel.
- **Step 3:** The water injection rate was subsequently increased in a step-wise manner (e.g. 0.02, 0.04, 0.8,...20 cm<sup>3</sup>/min). At each flow rate of water injection, we were observing the state of residual oil until no further oil blob mobilization was happening. At that time, a new picture was taken to calculate the reduced residual oil content; then the water injection rate was increased to a higher value for attained a further reduction of the residual oil content in the micromodel. Thus we collected enough data points for the amount of the residual oil remaining in place as a function of flow rate conditions.
- **Step 4:** To calculate the corresponding capillary number for each flow rate we had to calculate the Darcy velocity of water. This was determined by dividing the water flow rate by the cross-sectional area of the micromodel to fluid flow. The cross-sectional area for fluid flow was taken to be equal to the total width of the pore network (W) times 2D<sub>de</sub>, where D<sub>ep</sub> is the depth of pore etching. The corresponding capillary number was calculated using Equation (6).

The procedure for obtaining the capillary number curve for the displacement of continuous oil was as follows. High initial oil saturation was established as in **Step 1**. The micromodel was then flooded at a set water injection flow rate and a photograph was taken after there was no further oil movement in the micromodel. The model was then cleaned and re-saturated with water, followed by establishing high initial oil saturation again. Subsequently, the micromodel was waterflooded at a higher water injection rate. This was repeated again to collect 8 to 10 data points for generating the capillary number curve for the displacement of continuous oil.

### 3.3 Image analysis of residual oil

The residual oil remaining in place was determined by image analysis of the digital photographs taken at the end of each displacement condition [5]. The colored image of the micromodel with residual oil was converted into gray scale and then manual threshold was applied using the image analysis software so that the blobs in the threshold image appear to be the same size as the residual oil objects in place to the observer doing the analysis. Then the image analysis software reports the area of black objects (blobs) in the image. The maximum area of the blobs in the picture corresponded to the low capillary number displacement test, and for displacement tests at higher capillary number the area of blobs is smaller. It was assumed that the projected area of isolated oil blobs is proportional to the volume occupied, as the depth of etching is fairly constant [5]. Thus, we used the maximum area of the isolated blobs to normalize the residual oil fraction remaining in place at any given flow rate (or capillary number) condition. The term ( $S_{or}/S_{or}^*$ ), is the ratio of residual oil saturation established at a particular flow rate relative to the low capillary number waterflood residual oil saturation,  $S_{or}^*$ .

## 4. Experimental Results and Discussion

The advancement of the waterflooding process to the state of normal waterflood residual oil saturation attained at the lowest injection rate was monitored by video recording and still photos taken at various stages. Figure 4 illustrates that during waterflooding in a water-wet porous medium, there is a preferential selection of the relatively small pores where water imbibes and the trailing oil/water interfaces are in the relatively large pores. The residual oil is seen to be predominantly trapped in the larger pores in the pore network in the form of isolated oil blobs involving one to several pore bodies. Furthermore, the length of the oil blob structures tends to longer along the direction of displacement. Typical results obtained in our experiments conducted at the Institute's facilities for the residual oil remaining in place as a function of flow rate are as shown in Figure 5 for a small section of the micromodel SRC-1. After trapping the oil in this micromodel at an injection rate of  $0.1\text{cm}^3/\text{min}$ , the mobilization process was monitored by taking pictures at the end of each step-wise increase in water injection rate. As seen in the few pictures shown in Figure 5, there is very little change in the residual oil content as the flow rate was set at  $0.4\text{cm}^3/\text{min}$  although some oil blobs were locally mobilized a bit. However, at increased flow rates it is observed that the large residual oil blobs are broken-up into smaller segments and by the stage where the flow rate was  $5\text{cm}^3/\text{min}$  there are no branch like blobs any more. Further increase in flow rate causes more residual oil mobilization as well as more smearing of blobs creating sub-blob size oil droplets.

A display of the residual oil fraction remaining in place as a function of capillary number for the mobilization experiments using micromodel SRC-1 is shown in Figure 6. At a capillary number of about  $5 \times 10^{-5}$  we see some reduction of the normal waterflood residual oil saturation and for a capillary number greater than  $5 \times 10^{-4}$ , about half or more of the original residual oil has been mobilized. These results are in agreement with capillary number curves for mobilization of residual oil in sandstones reported in the literature. As seen in this plot, there is a significant mobilization of residual oil after we exceed a critical capillary number value.

Results of residual oil mobilization using micromodel SX-4 are shown in Figure 7. The characteristics of mobilization are very similar to those found in the mobilization experiments using micromodel SRC-1. Repeat experiments of mobilization of residual oil in micromodel SX-4 are very reproducible as seen from the results of runs 1 and 2 in Figure 7. Results obtained for the displacement of the continuous oil as a function of flow rate are shown in Figure 8. The residual oil remaining in place as a function of water injection rate for the displacement of initially continuous oil is similar to that for the mobilization experiment. There is a minor difference on the magnitude of residual oil remaining in place at the low flow rate-end for displacement of initially oil continuous case, as compared to the residual oil mobilization test, as this is evident from inspection of results shown for both cases. Therefore, there is some gain in oil recovery by waterflooding at higher capillary number for the oil initially being a continuous phase. At flow rates higher than  $1\text{cm}^3/\text{min}$  in the tests using the micromodel SRC-1, there appears to be no major difference between the two cases in the fraction of oil remaining in the micromodel. This behavior is also found to be in agreement with results in the published literature [2].

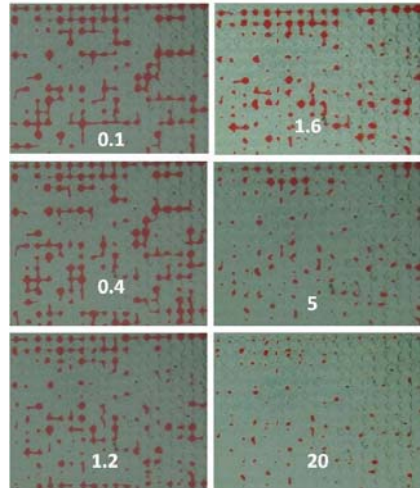


Figure 5. Details of the microstructure of residual oil left behind at different flow rates during mobilization tests in SRC-1. Number in picture indicates the flow rate of water in  $\text{cm}^3/\text{min}$ .

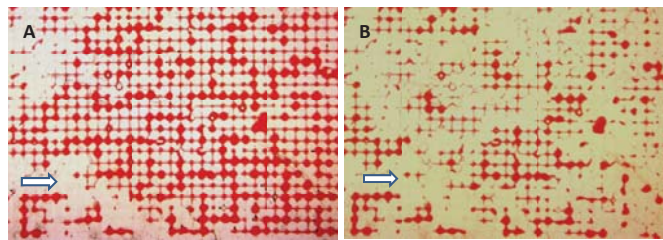


Figure 4. Illustration of the progress of the waterflooding process in model SX-4. Water was injected at constant rate invades the pore network filled with oil as shown. The water is a clear liquid imbibing along the direction shown by the arrow and the oil in pores is shown in red in stage A; b) The microscopic state of residual oil blobs after the end of low capillary number waterflooding is shown in stage B.

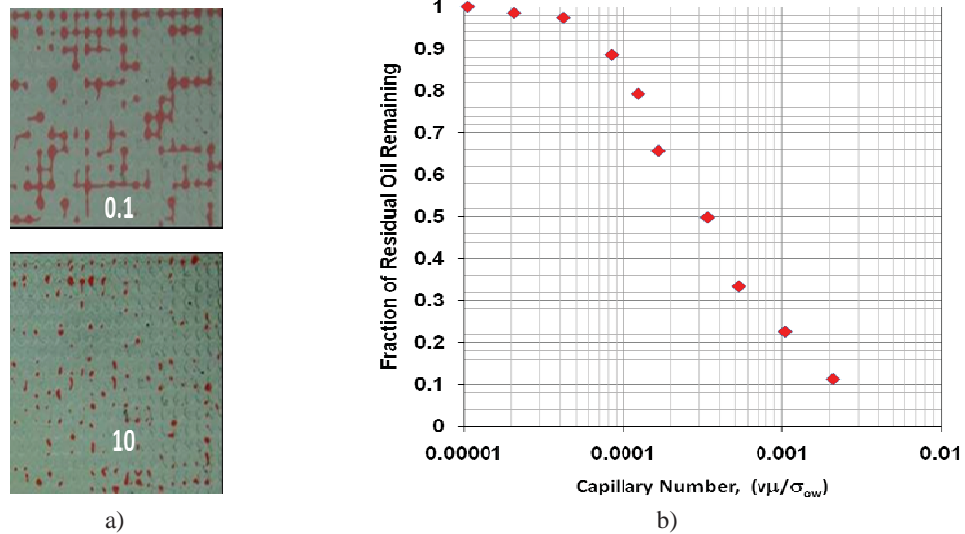


Figure 6. a) Visualization of the microscopic state of residual oil blobs in place at stages of mobilization with flow rates of 0.1 and 10  $\text{cm}^3/\text{min}$  in a 2-D glass micromodel with oil blobs shown in red; b) Capillary number curve for the fraction of residual oil remaining in place after mobilization at different capillary numbers.

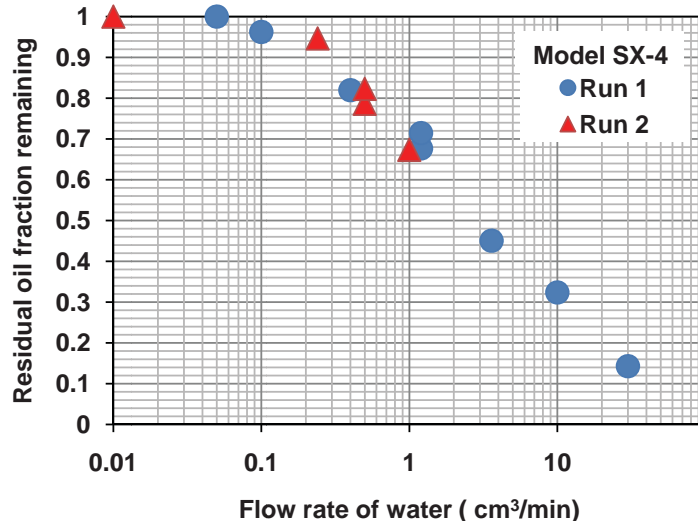


Figure 7. Mobilization of residual oil in micromodel SX-4.

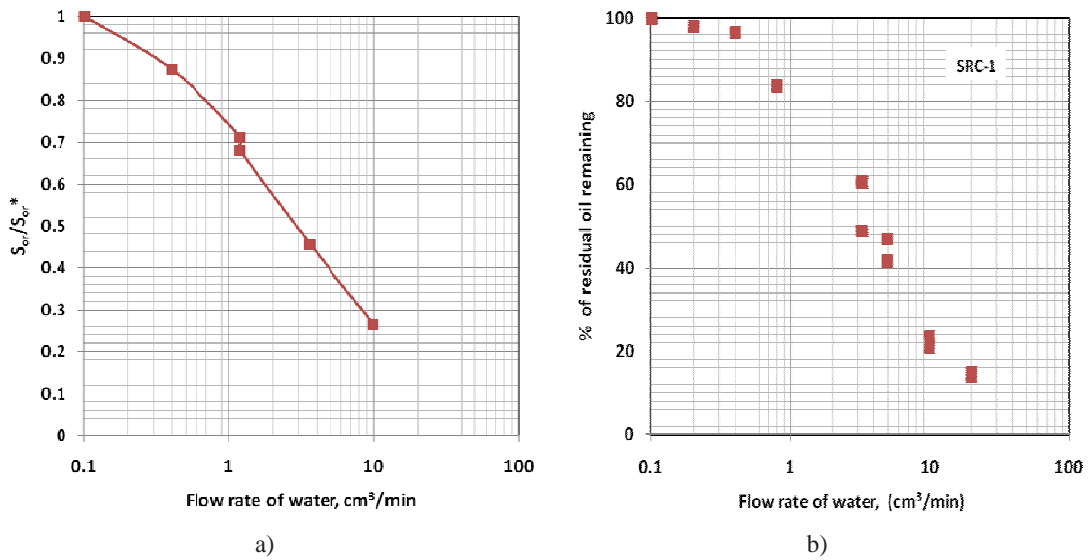


Figure 8. a) Displacement of initially continuous oil in SRC-1; b) Results for mobilization of residual oil in SRC-1.

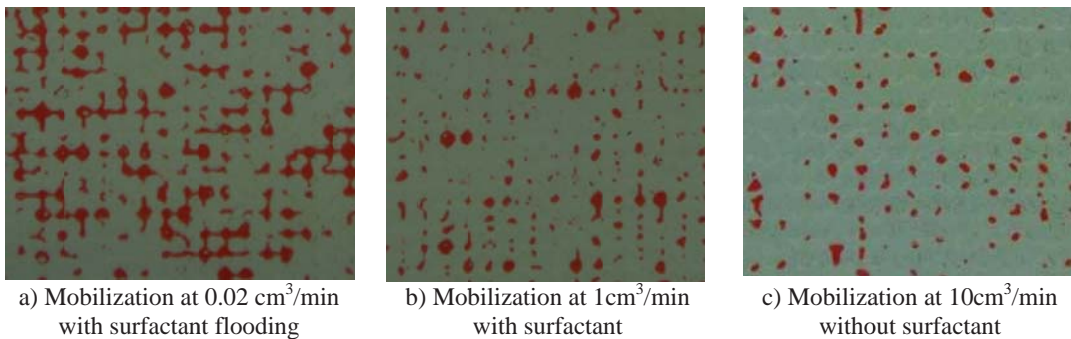


Figure 9. Microstructure of residual oil with surfactant and without surfactant flooding.

The effect of the oil-water interfacial tension was also examined. Figure 9 is a set of the pictures showing the residual oil microstructure at different conditions of waterflooding and mobilization. The surfactant was a hand -washing liquid in the laboratory. About 1wt% aqueous solution was made of it and this surfactant solution was injected as a slug in the inlet tube leading to the model's inlet fitting. This slug was driven into the micromodel by water injection at constant rate using the ISCO syringe pump. As it is seen from Figure 9, the very low injection rate surfactant flooding produced the residual oil microstructure which is similar to that obtained with much higher interfacial tension normal waterflooding shown in Figure 5 at the rate of  $0.1\text{cm}^3/\text{min}$ . Similarly, the state of residual oil remaining with surfactant flooding carried out at  $1\text{cm}^3/\text{min}$  and shown in Figure 9 is very similar to that obtained at no surfactant conditions with the flow rate at  $10\text{cm}^3/\text{min}$  shown in stage (c). These results are in qualitative agreement because the corresponding capillary numbers at these different velocities are the same for the low oil-water interfacial tension in surfactant flooding case compared to the capillary number corresponding to high flow rate mobilization without surfactant conditions [2].

When it comes to surfactant flooding at high capillary number, the residual oil that has not being swept away is seen to consist of tiny oil droplets of size smaller than the pore dimensions, yet this residual oil remains in place because of some finite contact angle they are attached to the pore walls. An example of this is the picture shown in Figure 10, taken with the micromodel under the microscope. It is evident that this type of residual oil remaining at a capillary number of about  $5 \times 10^{-3}$  is difficult to mobilize. For high capillary number conditions, there are locations in the water flow pathways that can retain attached to the pore walls these oil droplets. The water relative permeability at this condition approaches unity value, as reported in literature [4]. The results of this study have helped in providing direct evidence as to the reason why the relative permeability value to water at reduced residual oil conditions approaches unity at water saturations of 90% PV.

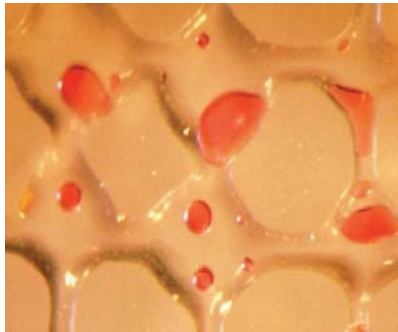


Figure 10. Close-up of oil droplets at high capillary number in SX-4. It is evident that this type of residual oil is very difficult to mobilize with water flowing past them.

## 5. Conclusions

The mobilization of residual oil observed in glass micromodels was made possible using image analysis to quantify the fraction of residual oil remaining in place at a constant injection rate of water. The capillary number curves obtained in this work are original and found to be in agreement with published results for water wet sandstones. It was also found that at capillary numbers greater than  $10^{-3}$ , the reduced residual oil is held in the pore space in the form of oil droplets that have a size normally smaller than the pore body size. These results demonstrate that micromodels have great potential for specialized core flooding tests and can be used to study various EOR processes in addition to oil blob mobilization.

## 6. References

1. I. Chatzis, N.R. Morrow and H.T. Lim, "Magnitude and Detailed Structure of Residual Oil Saturation", Soc. Petr. Eng. J. (April 1983), pp. 311-326.
2. I. Chatzis and N.R. Morrow, "Correlation of Capillary Number Relationships for Sandstones", Soc. Petr. Eng. J. (October 1984), pp. 555-562.
3. F. A. L. Dullien, Porous Media: Fluid Transport and Pore Structure, Academic Press, Second Edition, New York (1991).
4. N. R. Morrow, I. Chatzis, and H.T. Lim, "Relative Permeabilities at Reduced Residual Saturations," J. Cdn. Pet. Tech., **24** (Jul-Aug. 1985), pp. 62-69.
5. N. A. Sahloul, M. A. Ioannidis, and I. Chatzis: "Dissolution of non-aqueous phase liquids in porous media: pore scale mechanisms and mass transfer rates", Advances in Water Resources, **25(1)**, 2002, pp. 33-49.

### Acknowledgements

Mr. Bechir Mtawaa, Petroleum Engineering Program of the Petroleum Institute, is gratefully acknowledged for his assistance in providing access to the laboratory space used in this study as well as procuring an ISCO syringe metering pump.

### Author Biographies

**Mr. Ahmed Salah El Din Saad Ibrahim** is a Senior Student in the Petroleum Engineering Program at the Petroleum Institute. He has been involved in undergraduate research focused on EOR and on comparing Wireline and LWD logging. Mr. Ibrahim is a student member of the Society of Petroleum Engineers (SPE), and was selected to represent the Petroleum Institute at the SPE Student Paper Contest held in Doha in 2007.

**Mr. Nader Samir Abdelfattah** is a Senior Student in the Petroleum Engineering Program at the Petroleum Institute and is originally from Egypt. He aspires to become a reservoir engineer and is interested in EOR research. He is a student member of the SPE.

**Dr. Ioannis Chatzis** is a Visiting Distinguished Professor in the Department of Petroleum Engineering at the Petroleum Institute. He is sabbatical leave of absence for the entire year of 2008 from the University of Waterloo, Canada, where he is Professor of Chemical Engineering. He received all his degrees from the University of Waterloo (BASc 1974, MASc 1976, and Ph.D. 1980), which he joined in 1982 as a faculty member. He has supervised over 14 Ph.D. students and 24 Master's degree students. About half of his former Ph.D. students are now employed in academia, and the rest in research institutions. He teaches courses in Transport and Interfacial Phenomena, Reservoir Engineering, Flow in Porous Media, and Separation Processes. He is well known internationally for his research contributions on capillary and transport phenomena in porous media, with applications to pore structure characterization and novel EOR processes for the *in-situ* recovery of heavy oil from tar sand deposits. He has published extensively and has received the "Darcy" Technical Achievement Award of the International Society of Core Analysts in 2006 for his lifetime contributions to the field of Core Analysis. He is an inventor with three patents and co-author of a textbook titled "Introduction to Equilibrium Stage Separations".